974–982 *Nucleic Acids Research, 1997, Vol. 25, No. 5*

Multi-organ characterization of mitochondrial genomic rearrangements in ad libitum and caloric restricted mice show striking somatic mitochondrial DNA rearrangements with age

Simon Melov, Douglas Hinerfeld, Luke Esposito and Douglas C. Wallace*

Center for Genetics and Molecular Medicine, 1462 Clifton Rd., Emory University, Atlanta, GA 30322, USA

Received November 25, 1996; Revised and Accepted January 18, 1997

ABSTRACT

Mitochondrial DNA (mtDNA) rearrangements have been shown to accumulate with age in the post-mitotic tissues of a variety of animals and have been hypothesized to result in the age-related decline of mitochondrial bioenergetics leading to tissue and organ failure. Caloric restriction in rodents has been shown to extend life span supporting an association between bioenergetics and senescence. In the present study, we use full length mtDNA amplification by long-extension polymerase chain reaction (LX-PCR) to demonstrate that mice accumulate a wide variety of mtDNA rearrangements with age in post mitotic tissues. Similarly, using an alternative PCR strategy, we have found that 2–4 kb minicircles containing the origin of heavy-strand replication accumulate with age in heart but not brain. Analysis of mtDNA structure and conformation by Southern blots of unrestricted DNA resolved by field inversion gel electrophoresis have revealed that the brain mtDNAs of young animals contain the traditional linear, nicked, and supercoiled mtDNAs while old animals accumulate substantial levels of a slower migrating species we designate age-specific mtDNAs. In old caloric restricted animals, a wide variety of rearranged mtDNAs can be detected by LX-PCR in post mitotic tissues, but Southern blots of unrestricted DNA reveals a marked reduction in the levels of the age-specific mtDNA species. These observations confirm that mtDNA mutations accumulate with age in mice and suggest that caloric restriction impedes this progress.

INTRODUCTION

The application of PCR to detect mitochondrial DNA (mtDNA) deletions has revealed that mtDNA rearrangements accumulate with age in a number of organisms and tissues and correlates with individual senescence-specific mortality regardless of organismal maximum lifespan or metazoan phylum (1–13). Deleted mtDNAs have been observed to accumulate with age in a variety of postmitotic mammalian tissues (5,6,14,15). Duplications of mtDNA also accumulate (16). To date, most studies have used the PCR to detect the accumulation of single mtDNA rearrangements with age. In humans, the relative levels of deletion have been assessed primarily by quantitating the 'common' 5 kb deletion flanked by 13 bp direct repeats (1). However, studies of single mtDNA species may not be representative of the full extent of mtDNA damage. Consequently, we employed LX-PCR to amplify in one fragment 98% of the mitochondrial genome, through use of adjacent primers oriented in opposing directions (10). Application of this qualitative assay to aging human skeletal muscle has revealed that a spectrum of mtDNA rearrangements accumulates with age (10). Hence it would appear that a substantial portion of the mtDNAs becomes rearranged in skeletal muscle with age. These observations indicate that mtDNA rearrangements are at the very least, a reproducible biomarker of senescence.

It was previously reported that no substantive changes accumulate in the structure of the mitochondrial genome with age in either fibroblasts or *Drosophila melanogaster* (17,18). This was determined through analysis by Southern blot of uniquely restricted mitochondrial DNA. However, recent studies have shown that complex mtDNA rearrangements associated with human disease (19–21) can be 'masked' through restriction digestion (22). In addition, Southern analysis of unrestricted mtDNAs from senescent human skeletal muscle has revealed the accumulation of additional mtDNA species not found in young tissues which migrate with the same mobility as deleted mtDNAs (10). Hence, detection of age-specific mtDNA rearrangements requires application of appropriate methodologies.

Reactive oxygen species (ROS) including superoxide anion, hydrogen peroxide, and hydroxyl radical, generated within the mitochondria, have been hypothesized to play a major role in regulating rates of senescence both within, and between species (23–27). ROS production is reduced in isolated mitochondria in calorically restricted (CR) animals compared to ad-libitum (AL) fed animals (28). Attenuation of ROS production through CR is most pronounced in post-mitotic tissues such as brain and heart, and the levels of oxidative damage to lipids and proteins in CR animals is reduced when compared to AL fed animals (28).

*To whom correspondence should be addressed. Tel: +1 404 727 3346; Fax: +1 404 727 3949; Email: dwallace@gmm.gen.emory.edu

Therefore, mitochondrial ROS generation correlates with senescence, and genetic studies in a number of experimental aging models have confirmed that ROS generation is correlated with species-specific lifespan (28–31).

As a further step toward determining if mtDNA rearrangements play a significant role in senescence, it would be important to demonstrate that the accumulation of mtDNA rearrangements is retarded when mortality rate is reduced through genetic, or environmental modifications which extend lifespan. One of the few experimental aging models in which lifespan can be genetically extended is the *age-1* mutant of *Caenorhabditis elegans.* In this mutant, mtDNA rearrangements have been observed to accumulate at a slower rate than in wild-type animals (9). In mammals, the only reproducible treatment to date which extends lifespan is that of CR (32). When the total number of calories consumed by the animal is reduced over the lifespan relative to AL fed animals, the mean and maximum lifespan can be extended by up to 50% (33). The mechanism by which CR extends lifespan is unknown, but CR is associated with a decrease in total body fat, increased fitness, and decreased pathology.

In the present report, we have demonstrated that mtDNA rearrangements accumulate with age in mouse in multiple post-mitotic tissues. Moreover, in CR animals the extent of altered mtDNA in brain is attenuated relative to AL aged controls. Hence, mtDNA rearrangements may be functionally involved in the aging process.

MATERIALS AND METHODS

Mice

Female C57Bl/6JNia or C57Bl/6NNia mice were purchased from the NIA colonies of aging rodents at Charles River Laboratories Inc. Mice were categorized into three groups, young (2–4 months of age), old (32–35 months of age) and calorically restricted (32 months of age). Between five and seven animals were obtained for each age group or treatment (CR). Mice were housed for up to 2 weeks until sacrificed by cervical dislocation and their organs harvested and frozen at –80°C until DNA extraction.

DNA extraction and quantification

DNA was extracted from whole organs by standard techniques (34) with emphasis on minimizing shearing or nicking of DNA as nicked DNA has been shown to be refractory to LX-PCR (35). DNA from the brain was extracted from the right hemisphere. Extracted DNA was resuspended in 10 mM Tris 1 mM EDTA (pH 8) (TE) and stored at 4°C. A number of samples were normalized for mtDNA content by dot blotting and hybridization with digoxigenin-labeled full-length mtDNA and densitometry. In cases where mtDNA quantification was not carried out, the DNAs were normalized by A_{260} of total DNA.

Long Extension PCR (LX-PCR)

LX-PCR of mouse mtDNA employed primers: MSFlFor: TTT ATA GGC TAC GTC CTT CCA TGA GG (14520–14545) and MSFlRev: GGC AGG TAG GTC AAT GAA TGA GTG G (14207–14183) (36). These PCR primers were designed for LX-PCR and amplify 15983 bp of the mtDNA (Fig. 1) skipping only 312 bp of the *cytb* gene. Positive and negative controls were included for each PCR experiment.

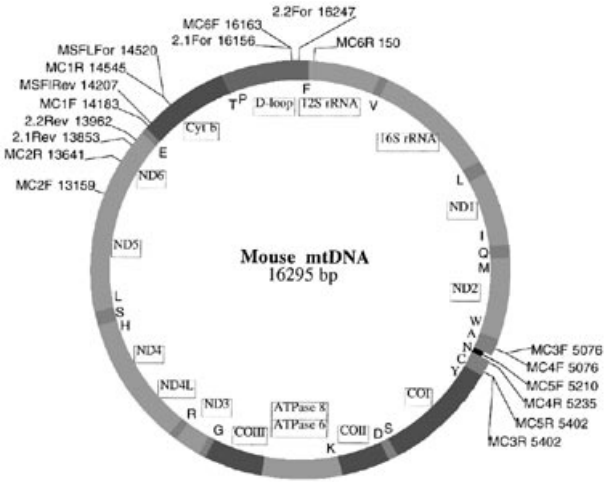

Figure 1. Mouse mitochondrial DNA map. tRNAs are listed by single letter abbreviation. Standard mitochondrial gene nomenclature is used. Primers used in various PCR assays are listed in their Forward (F) and Reverse (R) orientation. Numbers following primer identification refer to the 5′ end of the primer as described (36).

LX-PCR was carried out using the Boehringer Mannheim (Indianapolis, IN) Expand PCR kit. A biphasic hot start PCR reaction was performed using PCR gem 50 (Perkin Elmer, Foster City, CA), 0.2 μM primers (final concentration), 300 μM dNTPs, 1× Buffer 2, 1 U supplied enzyme/reaction, and either 100 ng of genomic DNA or 100 picograms (pg) of mtDNA (estimated by densitometry). The amplification was carried out in a total volume of 50 μl in thin walled microamp tubes (US Biochemical, Cleveland, OH) in a 9600 thermocycler (Perkin Elmer). The PCR profile involved an initial denaturation of 2 min, followed by a 2 step amplification of 35 cycles at 94°C (denaturation) for 10 s, and annealing/extension at 68°C for 10 min, followed by a final extension of 10 min at 72°C.

Specific mtDNA rearrangement PCR

After initial identification of mtDNA breakpoints by LX-PCR and sequence analysis, the PCR was used to amplify specific rearranged mtDNAs of different individuals from DNA of senescent heart. Two sets of primers were used: 2.1For: CTA TCA AAC CCT ATG TCC TG (16156–16175) plus 2.1Rev: CTG CTA TAG CTA CTG AGG AA (13853–13834) and 2.2For: CGT GAA CCA AAA CTC TAA TCA (16247–16267) plus 2.2Rev: AGT GGG TTT GTT GGT TGT TTA (13962–13942).

The PCR conditions were 0.2 μM primers (final concentration), 1 U Taq polymerase/reaction (Boehringer Mannheim), 1.5 mM Mg^{2+} (final concentration), 10 mM Tris–HCl (pH 8.3), 50 mM KCl, 200 μM dNTPs (Boehringer Mannheim) in a total volume of 50 μl. PCR was carried out in thin-walled PCR tubes (US Biochemical) in a 9600 PCR machine (Perkin Elmer) involving an initial denaturation of 2 min at 94°C, followed by 35 cycles of PCR at 10 s denaturation at 94°C, 30 s annealing at 54°C, 20 s extension at 72°C.

Minicircle PCR

To identify minicircles of mtDNA with >75% of their genome deleted, we devised an assay which uses PCR primers separated by between 100 and 500 bp with the 3′ ends oriented toward each

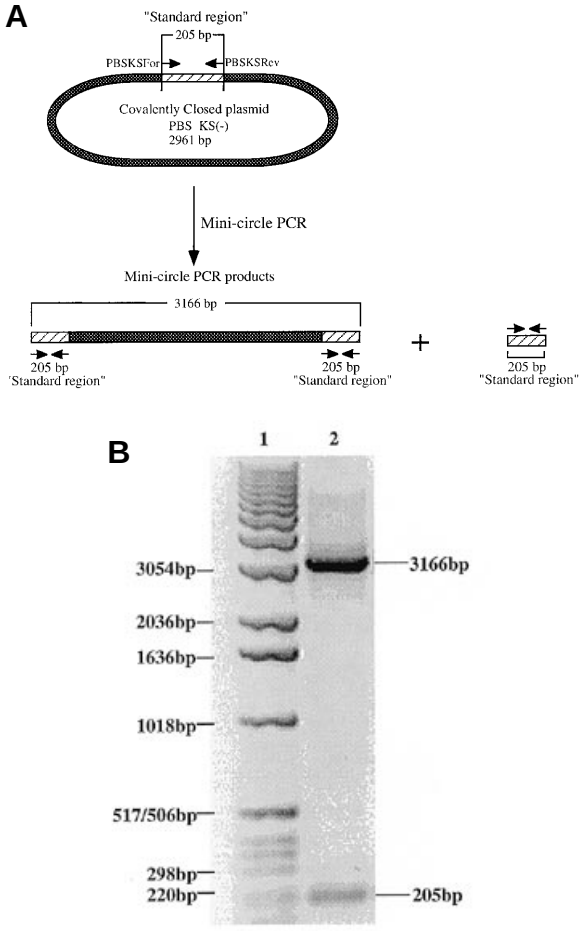

Figure 2. Minicircle PCR. (**A**) Diagram illustrating the principles of minicircle PCR. For every covalently closed molecule to which the primers anneal, three copies of the 'standard' region can be amplified (205 bp), one at either end of the large fragment, and one independently of the large fragment. (**B**) Example of minicircle PCR using PBS KS(–) a commercially available plasmid as target. Lane 1, molecular weight markers (Gibco/BRL 1 kb ladder); lane 2, 15% of minicircle PCR reaction products electrophoresed on a 1% agarose gel.

other (Fig. 2) but using an LX-PCR protocol with 10 min extension times. Replication is initiated at each primer extending past the opposing priming site and continues on around the covalently closed circle, past the initiating primer and ends at the opposing primer. This duplicates the entire covalently closed circle as well as the region bound by the PCR primers at either end of the completed PCR product. The amplification occurring between the region bound by the PCR primers serves as a positive control giving the 'standard' product (Fig. 2).

To demonstrate the validity of the minicircle amplification procedure, we amplified the 2.9 kb pBS KS(–) pBluescript plasmid (Stratagene, La Jolla, CA). Primers used were: PBSKSFor: CTT GGC GTA ATC ATG GTC ATA GCT GTT (797–823) and PBSKSRev: GCG TTG GCC GAT TCA TTA ATG CAG CT (1001–976), and the PCR conditions were 0.2 μM primers (final concentration) with 10 pg of purified PBS KS(–) (~10^6 copies) as target with all remaining conditions as described in LX-PCR. This amplification produced both the standard size PCR product together with a larger product equivalent in length to the entire pBluescript plasmid plus flanking repeats of the region between the two primers (Fig. 2B).

To determine which regions of the mouse mitochondrial genome were more likely to generate age-specific minicircles we evaluated a number of minicircle PCR primer pairs. These (M)ini-(C)ircle (F)orward and (R)everse (Fig. 1) were: MC1F: CCA CTC ATT CAT TGA CCT ACC TGC C (14183–14207) and MC1R: CCT CAT GGA AGG ACG TAG CCT ATA AA (14545–14520); MC2F: CCA GCA TTC CAG TCC TCA CAA TAC C (13159–13183) and MC2R: GCG GCA ATA TAT AGT TGT GCT ACT TG (13641–13616); MC3F: GCT AAG ACC TCA ACT AGA TTG GCA G (5076–5100) and MC3R: TCA GGC TCC GAA TAG TAG ATA GAG G (5402–5378); MC4F: GCT AAG ACC TCA ACT AGA TTG GCA G (5076–5100) and MC4R: CGA ATT GCA AAT TCG AAG GTG TAG AG (5235–5210); MC5F: CTC TAC ACC TTC GAA TTT GCA ATT CG (5210–5235) and MC5R: TCA GGC TCC GAA TAG TAG ATA GAG G (5402–5378); MC6F: ACC CTA TGT CCT GAT CAA TTC TAG TAG T (16163–16189) and MC6R: TAA GGG ATT TTA CAC CGG TCT ATG GA (150–125).

MtDNA minicircle PCR employed 100 ng of total DNA from young and senescent tissue using the above mentioned minicircle LX-PCR conditions.

Electrophoresis of PCR products

After completion of LX-PCR for rearrangements, or minicircle PCR, 30% of the PCR products were electrophoresed on a 0.8% or 1% agarose gel containing ethidium bromide (EtBr), with BRL 1 kb ladder standards (Gibco/BRL, Life Technologies, Gaithersburg, MD), lambda *Hin*dIII standards (Boehringer Mannheim) or BRL High Molecular weight standards (Gibco/BRL) and photographed electronically via EagleEye (Stratagene). Negative images of EtBr stained gels are used in this report as greater contrast is obtained.

Sequencing of mtDNA breakpoints

For sequencing of mtDNA rearrangement breakpoints, PCR products were excised from the gel with a sterile razor blade and the DNA extracted from the gel slice through use of a QIAquick gel extraction kit (Qiagen, Chatsworth, CA). In some instances, excised LX-PCR products were re-electrophoresed on a 3% agarose gel to further resolve DNA species before subsequent sequence characterization.

Cycle sequencing was carried out on gel purified PCR products with mtDNA primers according to Applied Biosystems Corporation (ABI, Division of Perkin Elmer) recommendations for use on an automated 373 or 377 ABI sequencer. Sequencing primers were synthesized and used to 'walk' along large regions in order to obtain continuous sequence from DNA fragments. Sequence analysis was carried out using Sequencher software (Gene Codes Corp., Ann Arbor, MI).

Field Inversion Gel Electrophoresis (FIGE) of total DNA, Southern blotting, and detection of mtDNA species

Total DNA was extracted from tissue and 15 μg was loaded onto 0.7% agarose gels containing EtBr. The gels were electrophoresed at 4°C in 40 mM Tris-Acetate 1 mM EDTA pH 8.3 (TAE) buffer at 2.6 V/cm for 70 h using FIGE conditions of 0.5 s forward direction, 0.25 second reverse direction. Buffer was replaced every 12 h throughout FIGE. After completion of the FIGE, the gel was photographed, denatured, neutralized and blotted overnight (34) onto positively charged nylon membrane (Boehringer Mannheim).

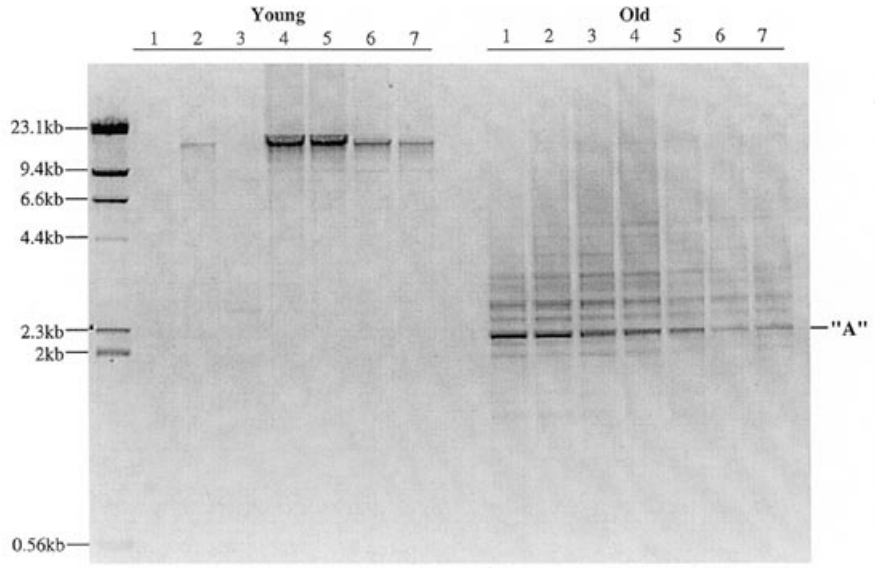

Figure 3. Relationship between quantity of target DNA and PCR products generated from LX-PCR of DNA from young and old heart. Young indicates mice 2 months of age, and Old indicates mice 32 months of age. Total heart DNA concentration used are: lane 1, 800 ng; 2, 400 ng; 3, 200 ng; 4, 100 ng; 5, 50 ng; 6, 25 ng; 7, 12.5 ng.

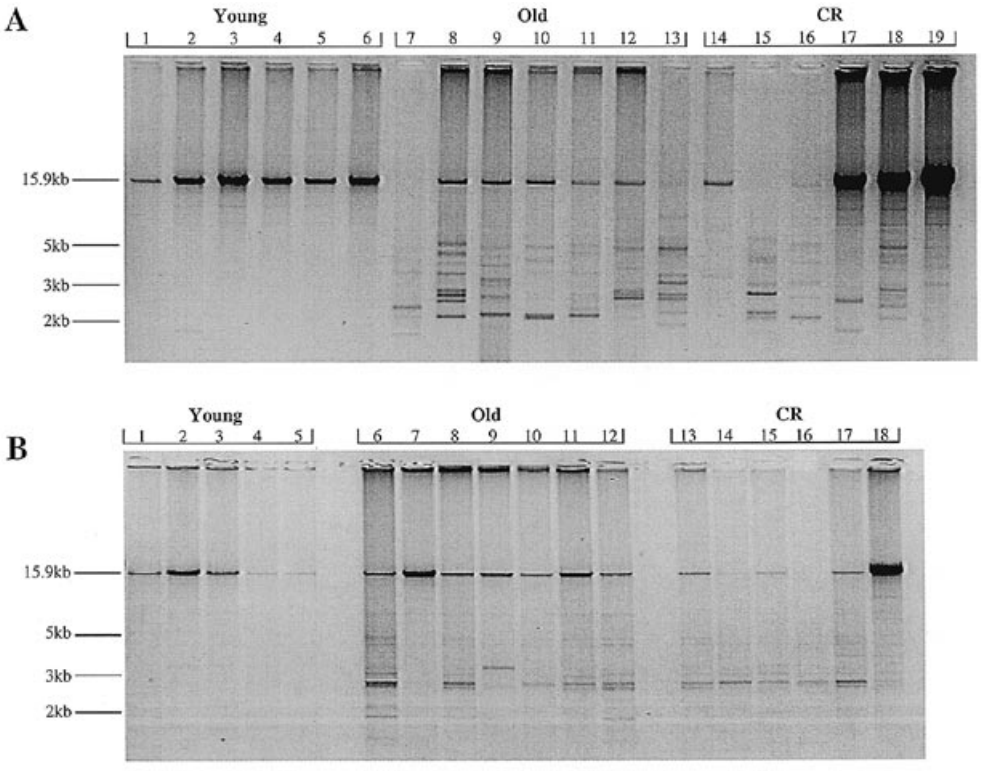

Figure 4. LX-PCR reaction product from young, old and Calorically Restricted (CR) animals; electrophoresed on a 0.8% agarose gel. (**A**) LX-PCR analysis of heart. Lanes 1–6, LX-PCR products from 2–4 month old mice; lanes 7–13, LX-PCR products of 32–35 month old mice; lanes 14–19, LX-PCR products of 32 month old CR mice. (**B**) LX-PCR analysis of brain. Lanes 1–5, LX-PCR products from 2–4 month old mice; lanes 6–12, LX-PCR products from 32–35 month old mice; lanes 13–18, LX-PCR products from 32 month old CR mice.

The mtDNA species were detected by hybridization of digoxigenin-labeled (Boehringer Mannheim), non-radioactive, mtDNA probe prepared from full-length LX-PCR amplified product. After washing and blocking, the signal was detected with the DIG Wash and Block Buffer Set, Anti-digoxigenin-AP Fab fragments, and CDP-*Star*™ (Boehringer Mannheim) to give lumigrams on XAR film (Eastman Kodak Co., Rochester, NY). Exposure of blots to film varied from 1 to 30 min dependent on the concentration of digoxigenin labeled mtDNA probe used in the hybridization.

Table 1.

mtDNA	AGE	5' Break point	Deleted Region	3' Break point	Region deleted	Primer pair
		16217		13785		
1	33mo#2	TATTTTAGTA	CTTGTAAAAA...ATCACCCCCA	ATACTAAAAA	13705	2.1kb
		87		13881		
2	33mo#2	GGTCCTGGCC	TTATAATTAA...ACCAACATCC	CCCCTAAATA	13793	2.2kb
		62		13822		
3	33mo#1	TTGTATCCCA	TAAACACAAA...TAGATCCCCA	AGTCTCTGGA	13759	2.1kb
		62		13649		
4	33mo#3	TTGTATCCCA	TAAACACAAA...CGCTACCCCA	ATCCCTCCTT	13586	2.1kb
		314		13781		
5	33mo#3	CGTGCCAGCC	ACCGCGGTCA...TATAATCACC	CCCAATACTA	13466	2.1kb
		173		13748		
6	33mo#4	AATTTAAGGA	GAGGGTATCA...ATAATAATTA	AGCACACAAA	13574	2.1kb
		16289		13355		
7	33mo#4	CAATAAACAT	TAACAAGTTA...CACCCATAAA	ATCTCTCAAC	13347	2.1kb
		314		13599		
8	33mo#1	CGTGCCAGCC	ACCGCGGTCA...AAAGATCACC	CAGCTACTAC	13284	2.1kb
		63		13828		
9	33mo#1	TGTATCCCAT	AAACACAAAG...CCCAAGTCTC	TGGATATTCC	13765	2.2kb
		52		13881		
10	32mo	AGATGGATAA	TTGTATCCCA...ACCAACATCC	CCCCTAAATA	13828	2.2kb
		214		13653		
11	32mo	ACACCTTGCC	TAGCCACACC...ACCCCAATCC	CTCCTTCCAA	13438	2.1kb
		80		13879		
12	33mo#2	AAGGTTTGGT	CCTGGCCTTA...CAACCAACAT	CCCCCCTAAA	13798	2.2kb

RESULTS

Rearranged mtDNA products detected by LX-PCR with age

To determine if mtDNA rearrangements accumulate with age in mice, LX-PCR was carried out on DNA extracted from liver, kidney, heart, and brain of young and old AL and old CR mice. The importance of the initial mtDNA concentration to the qualitative range of LX-PCR products was assessed by carrying out LX-PCR on whole tissue DNA samples normalized to the concentration of mtDNA by Southern blot hybridization or total DNAs normalized by optical density. No significant difference was observed in the range or level of rearranged species generated by LX-PCR for samples normalized by either of these methods (not shown). Consequently, most LX-PCR was carried out on DNA normalized by total DNA concentration.

To determine if the level of target DNA could significantly alter the number and nature of LX-PCR products, we also carried out LX-PCR analysis on serial dilutions of DNA targets as a control. Total DNAs extracted from a young heart (2 months of age) and from an old AL heart (33 months of age) were serially diluted starting at 800 nanograms (ng) and LX-PCR was carried out (Fig. 3). For DNA from young heart, optimal amplification of full-length mtDNA products occurred for target DNA concentrations between 100 and 12.5 ng. For DNA from old heart, amplification of full-length mtDNA was inhibited by the preferential amplification of rearranged mtDNAs at all higher target DNA concentrations. As the initial total DNA concentration is reduced, the number of rearranged mtDNA species increased until the maximum number of rearranged mtDNAs was seen at 100 ng of target DNA. The number of altered species subsequently declined with successive dilutions. These studies confirmed that LX-PCR products can be reproducibly detected over a wide range of DNA concentrations. Furthermore, particular species predominate in certain tissues such as the ~2 kb mtDNA species (species 'A', Fig. 3) which amplifies strongly from old heart tissue. The lack of amplification of full-length mtDNA by LX-PCR in some old individuals does not mean that there is a corresponding lack of full-length intact mtDNAs. Rather, the kinetics of LX-PCR will lead to preferential amplification of the shorter rearranged molecule.

The association between age and somatic mtDNA mutations was confirmed by analyzing the LX-PCR products from multiple young and old animals using a constant amount of total genomic DNA as template. A striking increase was observed in rearranged mtDNA of post mitotic tissues with age in all animals (Fig. 4). The accumulation of rearranged mtDNAs was most marked for DNA from heart and brain. LX-PCR of total DNA extracted from liver shows only a marginal increase in rearrangements with age (data not shown) and in kidney the predominant LX-PCR product was the full-length mtDNA regardless of age or caloric restriction (data not shown). Comparison of LX-PCR reactions between old individuals revealed that certain amplified products were consistently seen in a tissue. This is particularly noteworthy in DNA derived from brain (Fig. 4B). No qualitative difference in LX-PCR products was found between older CR mice and old AL mice in any tissue.

mtDNA breakpoint sequence characterization

Molecular sizing of LX-PCR products from DNA of 33 month old heart by high resolution gel electrophoresis revealed that species 'A' (Fig. 3) contained two products, a 2.1 and 2.2 kb species. Sequence analysis revealed each of these species contained unique mtDNA rearrangements (Table 1, mtDNAs 1 and 2). PCR primers were designed to specifically amplify across these mtDNA breakpoint junctions (2.1For and Rev, and 2.2For and Rev). DNA from old AL hearts of five individuals were analyzed, and the 2.1 and 2.2 kb primer sets were found to amplify a number of rearranged mtDNAs. Repeated PCR with the 2.1 kb primer set on the same old AL mouse heart repeatedly amplified a molecule with the same breakpoint (mtDNA 1, Table 1). Amplification using the same primer set on different animal DNAs resulted in amplification of rearranged molecules with different break points (data not shown). Of these, we characterized the breakpoints of a subset from five AL old hearts (Table 1, mtDNAs 3–12). PCR amplification of DNA from heart tissue of five young individuals detected no rearranged mtDNAs (data not shown).

The sequenced rearranged breakpoints proved to be heterogeneous. The rearranged mtDNAs 3 and 4 from different individuals had identical 5′ breakpoint ends but different 3′ ends. Both

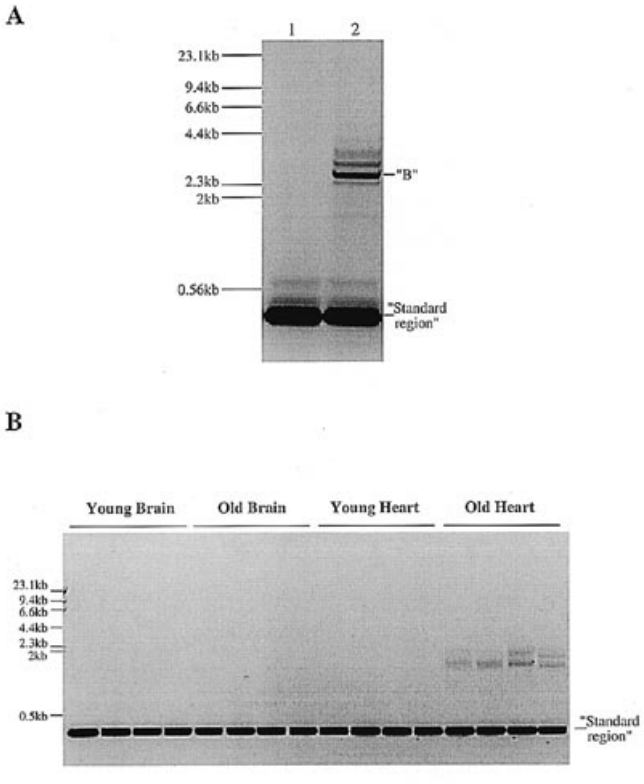

Figure 5. (**A**) Minicircle PCR on young and old heart total DNA. Lane 1, total DNA from heart of 2 months of age; lane 2, total DNA from heart of 33 months of age. (**B**) Minicircle PCR on young and old tissue from heart and brain.

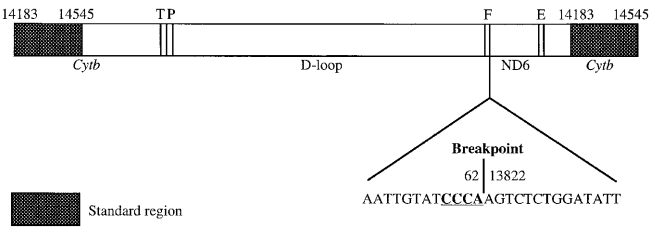

Figure 6. Molecular structure of a completely sequenced minicircle PCR product. Numbering of the mitochondrial genome is as described (36). The breakpoint junction encompasses 13 755 bp of the mitochondrial genome. The flanking repeat is underlined and in bold. Duplicated regions by the minicircle PCR assay are shaded.

breakpoints were flanked by the repeat CCCA (59–62) (Table 1). We identified direct repeats of two or more nucleotides at the 5′ and 3′ breakpoints in seven out of 12 breakpoints sequenced (underlined sequences in Table 1).

Minicircle PCR

Minicircle PCR amplification was applied to DNA from the individual hearts of several young and old animals. Using MC1 primers, senescent heart tissue was found to contain amplifiable minicircles (Fig. 5A). Using five other primer sets (MC2–6) on DNA from young and old tissues, minicircles were successfully amplified with MC6 primers, but not with primers MC2–5. Amplification using primer pair MC6 from heart and brain tissue DNA of four individuals each of the young and old age groups revealed minicircles only in the senescent heart tissue (Fig. 5B).

To further characterize the minicircles, we isolated from the gel the most prominent minicircle amplification product, an ~3 kb fragment we designate 'B' in Figure 5A. Although the 'B' DNA proved to contain a variety of different PCR products, further high resolution gel electrophoresis permitted isolation of a single species. The entire 2903 bp fragment of this minicircle was sequenced (Fig. 6). As expected, the minicircle sequence was flanked by a duplicated region, encompassing the MC1 primer pair. Therefore, the original minicircle with only one of the repeats was calculated to be 2540 bp. The breakpoint junction was between direct repeats present at 59–62 bp (CCCA) in the stem of the tRNA Phe, and 13 818–13 821 bp (CCCA) in ND6 removing 13 755 bp from the mtDNA and retaining only portions of the control region (D-loop), *cyt b*, ND6, and four tRNAs (Thr, Phe, Pro, Glu) (Fig. 6). The 5′ breakpoint junction identified in the minicircle PCR was identical to that sequenced and independently identified in rearranged mtDNAs 3 and 4, and has an identical 3′ breakpoint of rearranged mtDNA 3 (Table 1).

Analysis of the mtDNA structure from young, old and CR mice by Southern blot of unrestricted DNA

The conformational structures of the mtDNAs from young, old, and CR old animals was analyzed by Southern blotting and hybridization. MtDNA is a covalently closed circle, and reported to exist in a number of forms after isolation; supercoiled, nicked open-circular, and linear (37). The linear, supercoiled, and open-circular forms migrate in a characteristic pattern when electrophoresed in agarose gels containing EtBr. The linear species is the fastest migrating and corresponds with molecular size markers to the full length mitochondrial genome of 16.3 kb (Fig. 7, L). Supercoiled, and open-circular forms migrate more slowly (Fig. 7, SC, OC).

Analysis of mtDNAs from young and old post-mitotic heart by field inversion gel electrophoresis (FIGE), Southern blotting and detection of mtDNA species through hybridization with non-radioactive mtDNA probe, revealed a number of additional conformationally complex forms which migrate more slowly than OC mtDNA and are visible on lumigrams (Fig. 7). A number of these forms are common between all mtDNA samples from heart (Fig. 7A, lane 1 boxed region, indicated by an *). In addition, some of the heart DNAs from older animals had an Age-Specific (AS) species not seen in young AL or old CR animals (Fig. 7A, lane 6, boxed region), as well as a quantitative attenuation of some of the slower migrating (*) conformational forms. There are also a number of species which migrate faster than L mtDNA in certain hearts which remain uncharacterized (Fig. 7A). However, when comparing heart DNAs between young and old individuals, no substantial age specific trend was apparent (Fig. 7A). Qualitative assessment of liver and kidney mtDNAs by FIGE, Southern blotting, and hybridization of unrestricted mtDNA also failed to reveal age-associated differences between young, AL old and CR old samples (data not shown).

By contrast, analysis of brain mtDNAs revealed a dramatic change in the conformational forms of unrestricted mtDNA with age (Fig. 7B). An additional AS species of unknown size and form was consistently observed in the mtDNA of all old individuals (Fig. 7B, boxed region) but not in young. This AS form migrates just behind the supercoiled and open-circular

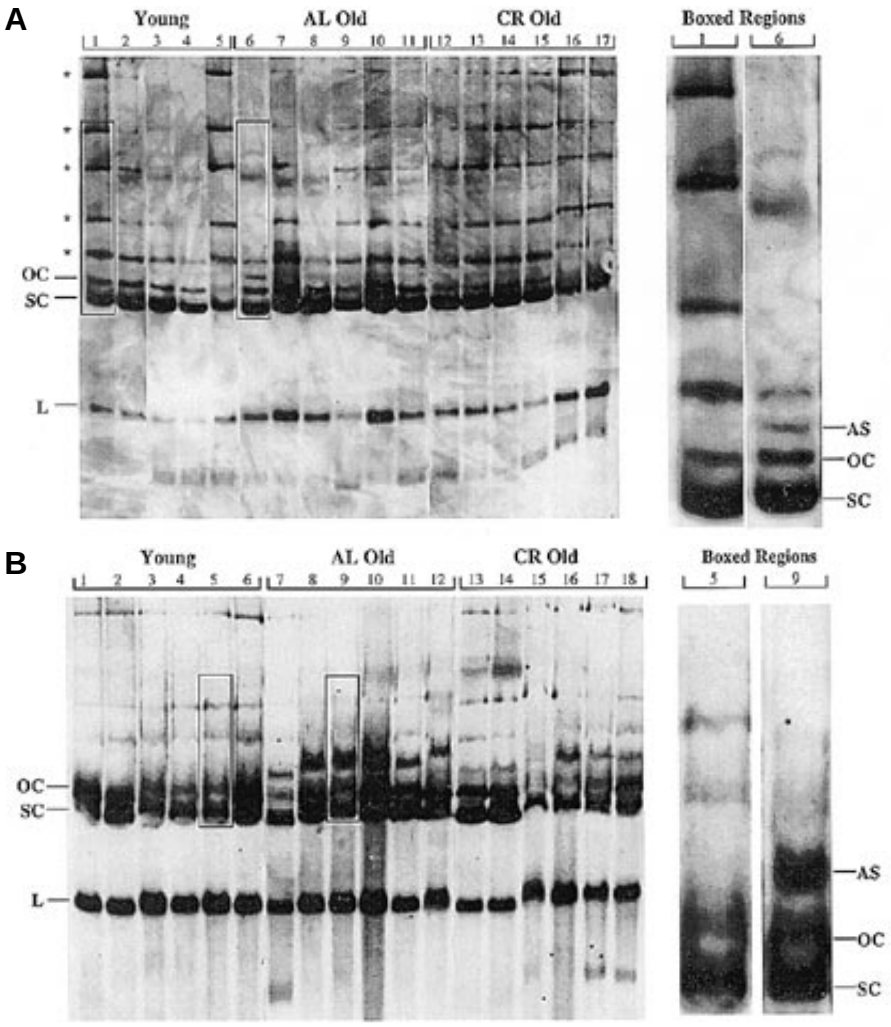

Figure 7. Southern blots of unrestricted mtDNA resolved by Field Inversion Gel Electrophoresis (FIGE). Total DNAs from young, Ad Libitum (AL) old and CR old are as described in Figure 4. (**A**) Heart mtDNA; (**B**) brain mtDNA. L, linear mtDNA; SC, supercoiled mtDNA; OC, open circular mtDNA; *common forms seen between samples. Boxed regions are enlarged to show detail of AS (Age Specific) molecular forms.

forms suggesting it may be a larger conformationally complex species. Hence, this species represents a clear age-specific change in the mtDNA of mouse brain.

The brain also appears to have more linearized mtDNA and fewer conformationally complex forms than heart. Prolonged exposures of young brain showed only four conformationally complex forms in comparison to the five conformational forms of mtDNA visible in young heart (data not shown). There is also a faster migrating species than linear mtDNA in the brains of some old and CR individuals (Fig. 7B, lanes 7, 17 and 18).

To determine if the brain AS mtDNA species was subject to the effects of CR, the same analysis was performed on DNA from old CR mouse brains. The AS species was found to be present but quantitatively attenuated in the CR group, appearing to be intermediate in intensity between young and old AL age groups (Fig. 7B).

DISCUSSION

The results of this study show that in post-mitotic tissues of the mouse there is an age-dependent accumulation of a heterogeneous array of mtDNA rearrangements. The mtDNA rearrangements observed in senescent heart vary in structure from individual to individual, while those found in senescent brain appear to present a more consistent 'pattern' between individuals of the same age. Either certain tissues have preferred rearrangements, or the PCR conditions employed preferentially amplify a specific subset of the rearranged mtDNAs from the brain samples. While LX-PCR is not a quantitative assay, it does reveal a dramatic qualitative difference in rearranged mtDNAs between young and old animals in post-mitotic tissues.

Sequence analysis of the breakpoint junctions of rearranged mtDNAs revealed that direct repeats are not a consistent feature of these somatic rearrangements. The absence of repeats flanking more mtDNA rearrangements indicates that they are not necessary for the rearrangement to occur. Analysis of age-related mtDNA deletions in rhesus monkeys has also shown that direct repeats are not a necessary requirement (8).

Our approach of amplifying virtually the whole genome rather than a specific rearrangement breakpoint provides a better overall indication of the range of mtDNA rearrangements. The identification of the same breakpoint in both the rearranged mtDNA PCR

product 3, and in a minicircle suggests that both assays can detect the same molecules from a particular tissue. Surprisingly, our methods have demonstrated that the tissue distribution of certain rearrangements is not uniform, with the minicircle PCR assay yielding comparatively few PCR products and only from senescent heart tissue. The results of the minicircle PCR assay indicates that senescent heart can accumulate deletions of the order of 13–14 kb for primer set MC1 and 14–15 kb for primer set MC6. Even though minicircles are confined to the heart, LX-PCR revealed deletions of 10–15 kb identified by the presence of 1.5–5 kb rearranged mtDNAs from AL old brain. Of the unique breakpoints identified by mtDNA rearrangement PCR, only products 5, 6, 8 and 11 would be capable of being detected in minicircle PCR using MC6 primers, as these priming sites are not removed in the remaining rearrangements. The fact that these large deletions do not yield products in minicircle PCR in the brain suggests that they are components of large and more complex rearrangements. Therefore it seems likely that age-specific minicircle mtDNAs are absent in the brain. In addition to the multiple mtDNA rearrangements identified by LX-PCR in post mitotic tissues, Southern analysis of unrestricted mtDNA revealed a unique conformational form in the brains of old AL animals relative to young. This form was reduced in CR animals.

Complex forms of mtDNA were first reported from HeLa cell mitochondria and human leukaemic leucocytes (37–40). By uni-directional gel electrophoresis, two additional species migrating slower than the open circular form have been observed in isolated mtDNA from dog cortex (41) and high molecular weight mtDNAs have been identified in HeLa cells (42). Additionally, complex forms of mtDNA including catenates and multiple monomeric units have been described in both cancerous and to a lesser extent aged tissues (11,38–40,43–46). In Kearns–Sayre syndrome (KSS), complex combinations of duplications and deletions have been described in the mtDNA from skeletal muscle biopsy (47). These types of complex mtDNA rearrangements may not be unique to human mitochondrial disease. Indeed, a head to tail unicircular dimer of mtDNA has been reported in mouse-L-cells and this is stable as a 32.6 kb molecule in cell culture (48). Further, examination of mtDNA from senescent mouse tissues by electron microscopy shows that there is an increase of between 0.2–3.3% of circular dimers with age (43). However, these levels are inadequate to account for the substantial amounts of conformationally altered forms of mtDNA we report here in AL old brain. It is therefore tempting to speculate that these conformationally complex forms may represent a combination of duplications and deletions.

The attenuation of the amount of conformational variant in the CR old brain is striking. Since the size and conformation of AS species is unknown, it is not possible to carry out densitometric analysis of these molecules relative to other forms of mtDNA (L, SC, and OC). However, the intermediate levels of AS species in older CR mice relative to young and AL old animals suggests it may be involved in senescence. Still, there are many biochemical parameters which change under the CR regimen, and it is conceivable that the AS form may be just another interesting biomarker of senescence.

Between 1 and 3% of total oxygen consumed by the mitochondria during normal respiration generates ROS (49). Age-specific increases in oxidative mtDNA damage have been demonstrated in a number of tissues and species (50–52). CR modulates the level of production of both hydrogen peroxide and superoxide anion ($O_2^{\cdot -}$) in senescent brain and heart. In senescent CR brain, the level of $O_2^{\cdot -}$ production is reduced by more than two-fold compared to AL old mice (53). In contrast, in CR old heart, levels of $O_2^{\cdot -}$ are only reduced by ~30% (53). If ROS are involved in causing mtDNA rearrangements, then the relative levels of ROS production in CR brain relative to heart are concordant with our observed levels of the AS conformational variants of mtDNA in these two tissues. The lack of substantial observable levels of AS forms of mtDNA detected by Southern blot from senescent heart and the concomitant detection of a heterogeneous array of rearranged mtDNAs and minicircles from the same tissue need not be mutually exclusive with the data we observed in mtDNA from brain. It is likely that the threshold of detection of rearrangements by the PCR assays is lower than that of Southern blots. It is intriguing that the only PCR primers with which we were able to successfully amplify minicircles were both in close proximity to the control region containing the origin of H-strand replication and the D-loop. Perhaps minicircles can be replicated in heart tissue. If so, then mtDNA damage may be relevant for functional decline in both heart and brain, but the molecular basis of mitochondrial dysfunction may be different.

It has often been hypothesized that quantitation of a single mtDNA deletion from old tissue represents 'the tip of the iceberg', and that the cumulative mitochondrial somatic mutational load is large in senescent organisms (1). By observing an array of mitochondrial sequence rearrangements with age, our data lend strong experimental support to this hypothesis. Further, the observation that there are substantial mtDNA conformational variants with age, and that the regimen of CR can modulate the level of the conformational variant in the brain, may indicate that mtDNA from the brain is more sensitive to oxidative damage as a result of ROS production. The current results in mouse are consistent with our previous studies in aging humans, in skeletal muscle (10), heart (15), and brain (5). The association of somatic mtDNA changes with age regardless of organismal maximum or mean lifespan, and modulation of some of these changes via CR, are consistent with the hypothesis that mtDNA changes with age may play a role in the senescence of multicellular organisms.

ACKNOWLEDGEMENTS

This work was supported by National Institutes of Health grant AG13154 and a Johnson and Johnson Focused giving grant awarded to D.C.W.

REFERENCES

1 Arnheim, N. and Cortopassi, G. (1992) *Mutat. Res.*, **275,** 157–167.
2 Baumer, A., Zhang, C., Linnane, A. W. and Nagley, P. (1994) *Am. J. Hum. Genet.*, **54,** 618–630.
3 Brossas, J. Y., Barreau, E., Courtois, Y. and Treton, J. (1994) *Biochem. Biophys. Res. Commun.*, **202,** 654–659.
4 Chung, S. S., Weindruch, R., Schwarze, S. R., McKenzie, D. I. and Aiken, J. M. (1994) *Aging Clin. Exp. Res.*, **6,** 193–200.
5 Corral-Debrinski, M., Horton, T., Lott, M. T., Shoffner, J. M., Beal, M. F. and Wallace, D. C. (1992) *Nature Genet.* **2,** 324–329.
6 Cortopassi, G. A. and Arnheim, N. (1990) *Nucleic Acids Res.*, **18,** 6927–6933.
7 Lee, C. M., Chung, S. S., Kaczkowski, J. M., Weindruch, R. and Aiken, J. M. (1993) *J. Gerontol.*, **48,** B201–205.
8 Lee, C. M., Eimon, P., Weindruch, R. and Aiken, J. M. (1994) *Mech. Ageing Dev.*, **75,** 69–79.
9 Melov, S., Lithgow, G. J., Fischer, D. R., Tedesco, P. M. and Johnson, T. E. (1995) *Nucleic Acids Res.*, **23,** 1419–1425.

10 Melov, S., Shoffner, J. M., Kaufman, A. and Wallace, D. C. (1995) *Nucleic Acids Res.*, **23,** 4122–4126.
11 Piko, L., Hougham, A. J. and Bulpitt, K. J. (1988) *Mech. Ageing Dev.*, **43,** 279–293.
12 Schwarze, S. R., Lee, C. M., Chung, S. S., Roecker, E. B., Weindruch, R. and Aiken, J. M. (1995) *Mech. Ageing Dev.*, **83,** 91–101.
13 Zhang, C., Baumer, A., Maxwell, R. J., Linnane, A. W. and Nagley, P. (1992) *FEBS Lett.*, **297,** 34–38.
14 Cortopassi, G. A., Shibata, D., Soong, N. W. and Arnheim, N. (1992) *Proc. Natl. Acad. Sci. USA*, **89,** 7370–7374.
15 Corral-Debrinski, M., Shoffner, J. M., Lott, M. T. and Wallace, D. C. (1992) *Mutat. Res.*, **275,** 169–180.
16 Lee, H. C., Pang, C. Y., Hsu, H. S. and Wei, Y. H. (1994) *FEBS Lett.*, **354,** 79–83.
17 White, F. A. and Bunn, C. L. (1985) *Mech. Ageing Dev.*, **30,** 153–168.
18 Calleja, M., Pena, P., Ugalde, C., Ferreiro, C., Marco, R. and Garesse, R. (1993) *J. Biol. Chem.*, **268,** 18891–18897.
19 Poulton, J., Deadman, M. E., Bindoff, L., Morten, K., Land, J. and Brown, G. (1993) *Hum. Mol. Genet.*, **2,** 23–30.
20 Poulton, J., Deadman, M. E. and Gardiner, R. M. (1989) *Nucleic Acids Res.*, **17,** 10223–10229.
21 Ballinger, S. W., Shoffner, J. M., Gebhart, S., Koontz, D. A. and Wallace, D. C. (1994) *Nature Genet.*, **7,** 458–459.
22 Poulton, J. and Holt, I. J. (1994) *Nature Genet.*, **8,** 313–315.
23 Bandy, B. and Davison, A. J. (1990) *Free Radic. Biol. Med.*, **8,** 523–539.
24 Ames, B. N. and Shigenaga, M. K. (1992) *Ann. NY Acad. Sci. 1992 Nov 21*, **663**: 85–96.
25 Ames, B. N. (1995) *Microbiologia*, **11,** 305–308.
26 Vanfleteren, J. R. (1993) *Biochem. J.*, **292,** 605–608.
27 Sohal, R. S. and Orr, W. C. (1992) *Ann. NY Acad. Sci. 1992 Nov 21*, **663**: 74–84.
28 Sohal, R. S., Ku, H. H., Agarwal, S., Forster, M. J. and Lal, H. (1994) *Mech. Ageing Dev.*, **74,** 121–133.
29 Agarwal, S. and Sohal, R. S. (1994) *Proc. Natl. Acad. Sci. USA*, **91,** 12332–12335.
30 Orr, W. C. and Sohal, R. S. (1994) *Science*, **263,** 1128–1130.
31 Vanfleteren, J. R. and De Vreese, A. (1995) *FASEB J.*, **9,** 1355–1361.
32 Weindruch, R. (1996) *Sci. Am.*, **274,** 46–52.
33 Weindruch, R. H., Walford, R. L., Fligiel, S. and Guthrie, D. (1986) *J. Nutrit.*, **116,** 641–654.
34 Sambrook, J., Fritsch, E. F. and Maniatis, T. (1989) *Molecular Cloning: A Laboratory Manual*, 2nd Ed. 3 vols., Cold Spring Harbor University Press, Cold Spring Harbor, NY.
35 Cheng, S., Chen, Y., Monforte, J. A., Higuchi, R. and Van Houten, B. (1995) *PCR Methods Appl.*, **4,** 294–298.
36 Bibb, M. J., Van Etten, R. A., Wright, C. T., Walberg, M. W. and Clayton, D. A. (1981) *Cell*, **26,** 167–180.
37 Hudson, B. and Vinograd, J. (1967) *Nature*, **216,** 647–652.
38 Clayton, D. A., Smith, C. A., Jordan, J. M., Teplitz, M. and Vinograd, J. (1968) *Nature*, **220,** 976–979.
39 Clayton, D. A. and Vinograd, J. (1967) *J. Pers.*, **35,** 652–657.
40 Hudson, B., Clayton, D. A. and Vinograd, J. (1968) *Cold Spring Harb Symp Quant Biol 1968*; **33**: 435–442.
41 White, B. C., Tribhuwan, R. C., Vander Laan, D. J., DeGracia, D. J., Krause, G. S. and Grossman, L. I. (1992) *J. Neurochem.*, **58,** 1716–1722.
42 Higuchi, Y. and Linn, S. (1995) *J. Biol. Chem.*, **270,** 7950–7956.
43 Bulpitt, K. J. and Piko, L. (1984) *Brain Res.*, **300,** 41–48.
44 Piko, L. (1992) *Ann N Y Acad Sci 1992 Nov 21*; **663**: 450–452.
45 Piko, L., Bulpitt, K. J. and Meyer, R. (1984) *Mech. Ageing Dev.*, **26,** 113–131.
46 Piko, L., Meyer, R., Eipe, J. and Costea, N. (1978) *Mech. Ageing Dev.*, **7,** 351–365.
47 Poulton, J., Morten, K. J., Marchington, D., Weber, K., Brown, G. K., Rotig, A. and Bindoff, L. (1995) *Muscle Nerve*, **3**, S154–158.
48 Bogenhagen, D., Lowell, C. and Clayton, D. A. (1981) *J. Mol. Biol.*, **148,** 77–93.
49 Chance, B., Sies, H. and Boveris, A. (1979) *Physiol. Rev.*, **59,** 527–605.
50 Hayakawa, M., Sugiyama, S., Hattori, K., Takasawa, M. and Ozawa, T. (1993) *Mol. Cell. Biochem.*, **119,** 95–103.
51 de la Asuncion, J. G., Millan, A., Pla, R., Bruseghini, L., Esteras, A., Pallardo, F. V., Sastre, J. and Vina, J. (1996) *FASEB J.*, **10,** 333–338.
52 Mecocci, P., MacGarvey, U., Kaufman, A. E., Koontz, D., Shoffner, J. M., Wallace, D. C. and Beal, M. F. (1993) *Ann. Neurol.*, **34,** 609–616.
53 Sohal, R. S., Agarwal, S., Candas, M., Forster, M. J. and Lal, H. (1994) *Mech. Ageing Dev.*, **76,** 215–224.